0022-3565/01/2971-410–422$3.00
THE JOURNAL OF PHARMACOLOGY AND EXPERIMENTAL THERAPEUTICS
JPET 297:410–422, 2001

Vol. 297, No. 1
3437/894550
Printed in U.S.A.

Metabolism of *levo*-α-Acetylmethadol (LAAM) by Human Liver Cytochrome P450: Involvement of CYP3A4 Characterized by Atypical Kinetics with Two Binding Sites

YUTAKA ODA and EVAN D. KHARASCH

Departments of Anesthesiology and Medicinal Chemistry, University of Washington, and the Puget Sound Veterans Affairs Medical Center, Seattle, Washington (E.D.K.); and Department of Anesthesiology, Osaka City University Medical School, Osaka, Japan (Y.O.)

Received October 13, 2000; accepted January 2, 2001 This paper is available online at http://jpet.aspetjournals.org

ABSTRACT

levo-α-Acetylmethadol (LAAM) is a long-acting opioid agonist prodrug used for preventing opiate withdrawal. LAAM undergoes bioactivation via sequential *N*-demethylation to nor-LAAM and dinor-LAAM, which are more potent and longer-acting than LAAM. This study examined LAAM and nor-LAAM metabolism using human liver microsomes, cDNA-expressed CYP, CYP isoform-selective chemical inhibitors, and monoclonal antibody to determine kinetic parameters for predicting in vivo drug interactions, involvement of constitutive CYP isoforms, and mechanistic aspects of sequential *N*-demethylation. *N*-Demethylation of LAAM and nor-LAAM by human liver microsomes exhibited biphasic Eadie-Hofstee plots. Using a dual-enzyme Michaelis-Menten model, K_m values were 19 and 600 μM for nor-LAAM and 4 and 450 μM for dinor-LAAM formation, respectively. LAAM and nor-LAAM metabolism was inhibited by the CYP3A4-selective inhibitors troleandomycin, erythromycin, ketoconazole, and midazolam. Of the cDNA-expressed isoforms examined, CYP2B6 and 3A4 had the highest activity toward LAAM and nor-LAAM at both low (2 μM) and high (250 μM) substrate concentrations. *N*-Demethylation of LAAM and nor-LAAM by expressed CYP3A4 was unusual, with hyperbolic velocity curves and Eadie-Hofstee plots and without evidence of positive cooperativity. Using a two-site model, K_m values were 6 and 0.2 μM, 1250 and 530 μM, respectively. Monoclonal antibody against CYP2B6 inhibited CYP2B6-catalyzed but not microsomal LAAM or nor-LAAM metabolism, whereas troleandomycin inhibited metabolism in all microsomes studied. The ratio [dinor-LAAM/(nor-LAAM plus dinor-LAAM)] with microsomes and CYP3A4 decreased with increasing LAAM concentration, suggesting most dinor-LAAM is formed from released nor-LAAM that subsequently reassociates with CYP3A4. Based on these results, we conclude that LAAM and nor-LAAM are predominantly metabolized by CYP3A4 in human liver microsomes, and CYP3A4 exhibits unusual multisite kinetics.

levo-α-Acetylmethadol (LAAM) is an analog of methadone characterized by equieffective and longer duration of action (Fraser and Isbell, 1952; Eissenberg et al., 1999). LAAM is effective when administered orally every 2 or 3 days, and was recently approved as an alternative to methadone for opiate maintenance therapy (Rawson et al., 1998). Although LAAM has μ-receptor agonist activity, it is functionally a prodrug with a long duration of effect attributed primarily to sequential *N*-demethylation to the secondary amine nor-LAAM and the primary amine dinor-LAAM (Billings et al., 1973; Walsh et al., 1998). Nor-LAAM is 15 to 200 times more potent than LAAM based on in vitro binding assays (Nickander et al., 1974; Horng et al., 1976; Walczak et al., 1981), and 6 to 12 times more potent in vivo (Vaupel and Jasinski, 1997). Dinor-LAAM is approximately 10 times, and 1.5 to 3 times more potent than LAAM based on in vitro binding assays (Nickander et al., 1974; Horng et al., 1976) and an investigation in dogs (Vaupel and Jasinski, 1997), respectively, although other in vitro and in vivo investigations have suggested it is less potent than LAAM (Smits, 1974; Walczak et al., 1981). In addition to greater potency, nor-LAAM and dinor-LAAM are eliminated more slowly than LAAM. The elimination half-life of LAAM, nor-LAAM, and dinor-LAAM are approximately 0.5, 1 to 1.5, and 3 to 4 days, respectively, in humans (Kaiko and Inturrisi, 1975; Henderson, 1976; Walsh et al., 1998). In humans, the clinical onset of LAAM was slower after intravenous than after oral administration, when first-pass metabolism can occur (Fraser and Isbell, 1952) and was correlated more with nor-LAAM than with LAAM plasma concentration (Kaiko and Inturrisi, 1975). Nonetheless, a recent investigation showed that LAAM itself can contribute

This study was supported by a Merit Review Award from the Veterans Affairs Medical Research Bureau and National Institutes of Health Grant K24DA00417.

ABBREVIATIONS: LAAM, *levo*-α-acetylmethadol; CYP, cytochrome P450; cDNA, complementary deoxyribonucleic acid; DDC, diethyldithiocarbamate; TAO, troleandomycin; HPLC, high performance liquid chromatography; HLM, human liver microsome; AIC, Akaike's information criterion; E, enzyme; S, substrate; CL, clearance.

to the pharmacological effect of the parent drug (Walsh et al., 1998).

Understanding the clinical effects of LAAM, therefore, requires a comprehensive elucidation of the pharmacokinetics and pharmacodynamics of the drug and its metabolites. In addition, induction and inhibition of *N*-demethylation may substantially alter the disposition and clinical effect of LAAM. However, there have been few investigations of LAAM drug interactions. Effects of phenobarbital induction on LAAM and metabolites disposition were evaluated in rats (Roerig et al., 1977; Kuttab et al., 1985). There are no investigations elucidating the effects of drug interactions on the metabolism of LAAM in humans.

In the absence of in vivo data, in vitro metabolism is often used to predict the consequences of clinical drug interactions (Houston and Carlile, 1997; Obach et al., 1997). Moody et al. (1997) showed that cytochrome P450 (CYP) 3A4 was a predominant isoform involved in the *N*-demethylation of LAAM and nor-LAAM in human liver microsomes in vitro. There are wide interindividual variations in CYP3A4 activity and CYP3A4 susceptibility to drug interactions that influence the pharmacokinetics of various agents in vivo (Shimada et al., 1994; Dresser et al., 2000). Also, CYP3A4 in intestine, as well as in liver, significantly contributes to the metabolism of CYP3A4-mediated drugs administered orally (Kolars et al., 1991; Paine et al., 1996). Although CYP3A4 has been identified as metabolizing LAAM and nor-LAAM in vitro (Moody et al., 1997), there have been, to our knowledge, no reports determining the Michaelis-Menten kinetic parameters for metabolism, which are essential for elucidating the contribution of CYP3A4 in the metabolism of LAAM and the metabolic interactions between LAAM and nor-LAAM with other agents. In addition, the role of CYP2B6, which has been increasingly recognized as metabolizing numerous CYP3A4 substrates (Ekins and Wrighton, 1999), in the metabolism of LAAM and nor-LAAM, is unknown. The aim of the present study is to determine the CYP isoforms and produce kinetic models based on the Michaelis-Menten kinetic parameters for the metabolism of LAAM and nor-LAAM using human liver microsomes, complementary DNA (cDNA)-expressed CYP isoforms, CYP isoform-specific chemical inhibitors, and monoclonal antibody in vitro.

Materials and Methods

Chemicals. LAAM·HCl (d_0), deuterated LAAM·HCl {(−)-[1,1,1,2,2,3-$^2H_6$]-α-acetylmethadol·HCl} (d_6), nor-LAAM·HCl (d_0), deuterated nor-LAAM·HCl {(−)-[1,1,1,2,2,3-$^2H_6$]-α-acetyl-*N*-normethadol·HCl} (d_6), dinor-LAAM·HCl (d_0), and deuterated dinor-LAAM·HCl {(−)-[acetyl-$^2H_3$]-α-acetyl-*N*,*N*-dinormethadol·HCl} (d_3) were prepared at Research Triangle Institute (Research Triangle Park, NC) and provided by the National Institute on Drug Abuse (Rockville, MD). Glucose 6-phosphate, glucose-6-phosphate dehydrogenase (type VII), β-nicotinamide adenine dinucleotide phosphate, 8-methoxypsoralen, orphenadrine, paclitaxel, diclofenac, quinidine hydrochloride, diethyldithiocarbamate (DDC), troleandomycin (TAO), erythromycin, ketoconazole, and midazolam were purchased from Sigma Chemical Co. (St. Louis, MO). Furafylline and sulfaphenazole were obtained from Ultrafine Chemicals (Manchester, UK). Human liver tissue medically unsuitable for transplant was obtained from University of Washington Medical Center (Seattle, WA). cDNA-expressed CYP isoforms in microsomes and monoclonal antibody against CYP2B6 were obtained from Gentest Corp. (Woburn, MA). Acetonitrile (HPLC grade) was purchased from J.T. Baker (Phillipsburg, NJ). Unless specified, all other reagents were purchased from Sigma Chemical Co. and were of the highest purity available. All buffers and reagents were prepared with high-purity (18.2 MΩ · cm) water (Milli-Q; Millipore, Bedford, MA).

Incubation Conditions with Human Liver Microsomes and cDNA-Expressed Human CYP Microsomes. Microsomes were prepared from human liver by differential centrifugation of homogenates as described by Kharasch and Thummel (1993), and stored at −80°C until used. Protein concentration of the microsomal fractions was measured using the method of Lowry et al. (1951), with bovine serum albumin as standard. P450 content was determined from the difference spectrum of carbon monoxide-reduced versus oxidized microsomes as described by Omura and Sato (1964). Incubations were conducted at a final volume of 1.0 ml in 100 mM potassium phosphate buffer (pH 7.4) containing human liver microsomes (0.1 mg of protein) and LAAM or nor-LAAM (0.05–1000 μM). The incubation mixture was preincubated at 37°C for 3 min, initiated by addition of the NADPH generating system (final concentrations: 10 mM glucose 6-phosphate, 1.0 mM NADP, and 1.0 units of glucose-6-phosphate dehydrogenase and 5 mM magnesium chloride, preincubated at 37°C to preform NADPH) and terminated after 10 min by addition of 0.2 ml of 20% trichloroacetic acid and placing in an ice-water bath. Experiments with the constitutive human liver CYP isoforms CYP1A2, 2A6, 2B6, 2C8, 2C9, 2C19, 2D6, 2E1, 3A4, and 3A5 were done as described above, except 10 pmol of cDNA-expressed CYP isoforms was used instead of microsomes and incubation was for 30 min. Metabolic activity of CYP3A4 was examined with and without coexpressed cytochrome b_5. Formation of metabolites was detected following incubation of substrates with control microsomes without expression of CYP isoforms and this activity was used as blanks.

Inhibition with Monoclonal Antibody and CYP Isoform-Specific Inhibitors. Experiments with monoclonal antibody against CYP2B6 were conducted with preincubation of antibody (0.02 mg of protein) with microsomes (0.05 mg of protein) on ice for 15 min, followed by preincubation with the substrate in potassium phosphate buffer at 37°C for 3 min and the reaction was started by the addition of NADPH generating system and lasted for 10 min. Samples incubated with trishydroxymethylaminomethane, the solvent of the antibody, without antibody were used as controls. Characterization, specificity, and inhibition activity of this antibody have been reported by others (Roy et al., 1999; Huang et al., 2000). Experiments with isoform-selective CYP inhibitors were conducted at the following final concentrations with microsomes from two individuals (HLM158 and 167); inhibitor concentrations were chosen to inhibit >80% of CYP isoform activity (Kharasch and Thummel, 1993; Koenigs et al., 1997; Nadin and Murray, 1999): furafylline (CYP1A2 inhibitor), 30 μM; 8-methoxypsoralen (CYP2A6), 2.5 μM; orphenadrine (CYP2B6), 50 μM; paclitaxel (CYP2C8), 250 μM; diclofenac (CYP2C8 and 9), 250 μM; sulfaphenazole (CYP2C9), 10 μM; quinidine (CYP2D6), 5 μM; DDC (CYP2E1), 100 μM; TAO (CYP3A4), 100 μM; erythromycin (CYP3A4), 100 μM; ketoconazole (CYP3A4), 5 μM; and midazolam (CYP3A4), 100 μM. All inhibitors were diluted in methanol (final methanol concentration 1%) except orphenadrine, diclofenac, and DDC, which were added in potassium phosphate buffer. The concentration of both LAAM and nor-LAAM was 5 μM. The effect of TAO was also examined at 1 μM LAAM and 0.2 mg of protein (HLM135) for measuring remaining LAAM and formation of nor-LAAM and dinor-LAAM. In experiments using the competitive inhibitors paclitaxel, diclofenac, sulfaphenazole, quinidine, ketoconazole, and midazolam, the inhibitor was added to the incubation mixture with substrate, preincubated at 37°C for 3 min, and the reaction was initiated by the addition of the NADPH generating system. Reactions were carried out at 37°C for 10 min and then terminated with trichloroacetic acid as described above. Incubations containing the mechanism-based inhibitors furafylline, 8-methoxypsoralen, orphenadrine, DDC, TAO, or erythromycin were first preincubated at 37°C for 15 min with microsomes and NADPH generating system, and then the substrate was added to start the reaction.

Analytical Determinations. After termination of the incubation, deuterated internal standards of nor-LAAM (d_6, 72.5 pmol) and dinor-LAAM (d_3, 7.6 pmol) were added to the samples. LAAM (d_6, 696 pmol) was also added to measure the remaining LAAM. Samples were then applied to an MCX extraction column (Waters, Milford, MA) and passed through at a flow rate of 1.5 ml/min. The MCX column was first washed with 1 ml of 0.1 N hydrochloric acid followed by 1 ml of methanol. The retained compounds were eluted with 1 ml of methanol/30% ammonium hydroxide (95/5, v/v). The eluates were dried under nitrogen, reconstituted in 50 μl of HPLC mobile phase. Five microliters of the reconstituted residues was injected into the HPLC (Series 1100 MSD; Agilent Technologies, Wilmington, DE) fitted with a Zorbax Eclipse XDB-C18 column (2.1 $\times$ 50 mm, 5-μm particle size; Agilent Technologies) and a Zorbax Eclipse XDB guard column (2.1 $\times$ 12.5 mm, 5 μm) with an isocratic mobile phase of 38% acetonitrile in 20 mM ammonium acetate (pH 6.9). The mass spectrometer was equipped with an electrospray interface and was operated in the positive ionization mode. The interface was maintained at 325°C with a nitrogen nebulization pressure of 20 psi, resulting in a flow of 6.0 l/min. Detection was performed at *m/z* 326.2, 329.2, 340.2, 346.2, 354.2, and 360.2 for dinor-LAAM (d_0), dinor-LAAM (d_3), nor-LAAM (d_0), nor-LAAM (d_6), LAAM (d_0), and LAAM (d_6), respectively, with 80-V fragmentation. Retention times of dinor-LAAM (d_0), dinor-LAAM (d_3), nor-LAAM (d_0), nor-LAAM (d_6), LAAM (d_0), and LAAM (d_6) were 4.30, 4.28, 5.60, 5.51, 8.45, and 8.28 min, respectively. The peak area ratios, d_0/d_6 of LAAM, d_0/d_6 of nor-LAAM, and d_0/d_3 of dinor-LAAM were used to calculate concentrations based on least-squares regression of calibrators (50–5000 pmol/ml for LAAM, 5–5000 pmol/ml for nor-LAAM, and 0.5–500 pmol/ml for dinor-LAAM) included in each run. Metabolites of LAAM or nor-LAAM were not detected in blank samples without NADPH or substrates. The lower limit of quantitation was 0.5 pmol/ml for LAAM, nor-LAAM, dinor-LAAM, and the intra-assay and interassay variations were less than 7% throughout the range.

Prediction of in Vivo Formation Clearance of Nor-LAAM and Dinor-LAAM. Predicted effects of enzyme induction and inhibition on in vivo formation clearances of nor-LAAM and dinor-LAAM were calculated using 3-fold increases and decreases in V_{max}. In vivo clearance was scaled from the microsomal V_{max}/K_m using the following scaling factor: 45 mg of microsomal protein per gram of liver and 20 g of liver per kilogram of body weight (Houston, 1994; Carlile et al., 1999).

Data Analysis. Microsomal velocity versus substrate concentration data were analyzed using a dual-enzyme Michaelis-Menten model. This model was selected because hyperbolic Eadie-Hofstee curves most often indicate multiple CYP isoforms participation in microsomal reactions. In the following equations, S is the substrate concentration; K_{m1} and K_{m2}, high- and low-affinity Michaelis-Menten constants, respectively; V_{max}, maximum metabolic velocity; V_{max1} and V_{max2}, high- and low-affinity maximum metabolic velocity, respectively; K', binding constant; and n, number of binding sites.

$$V = \frac{V_{max1} \cdot S}{K_{m1} + S} + \frac{V_{max2} \cdot S}{K_{m2} + S} \quad (1)$$

CYP3A4 data were analyzed using several models, based on the recognition that this isoform contains at least two binding sites (Korzekwa et al., 1998; Shou et al., 1999; Hosea et al., 2000). If the binding sites are nonindependent and exhibit cooperativity, then the general allosteric model (Hill equation) can be used, with known limitations (Shou et al., 1999).

$$V = \frac{V_{max} \cdot S^n}{K' + S^n} \quad (2)$$

A cooperative single-enzyme model with two binding sites in which product can be formed either from the single-substrate-bound form (ES) or from the two-substrate-bound form (ESS) of the enzyme was described by Korzekwa et al. (1998).

$$V = \frac{\frac{(V_{max1} \cdot S}{K_{m1}} + \frac{V_{max2} \cdot S^2}{K_{m1} \cdot K_{m2}}}{\left(1 + \frac{S}{K_{m1}} + \frac{S^2}{K_{m1} \cdot K_{m2}}\right)} \quad (3)$$

If $K_{m2} \gg K_{m1}$ and $S \ll K_{m2}$ this reduces to the following:

$$V = \frac{(V_{max1} \cdot S) + \left(\frac{V_{max2}}{K_{m2}}\right) \cdot S^2}{(K_{m1} + S)} \quad (4)$$

where (V_{max2}/K_{m2}) is modeled as a single parameter.

If the enzyme and substrate can form an ES complex or an ESS complex, but only the ESS complex results in product formation, then $V_{max1} = 0$ and eq. 3 reduces to the following:

$$V = \frac{\left(\frac{V_{max2} \cdot S^2}{K_{m1} \cdot K_{m2}}\right)}{\left(1 + \frac{S}{K_m} + \frac{S^2}{K_{m1} \cdot K_{m2}}\right)} \quad (5)$$

When $K_{m2} \gg K_{m1}$ and $V_{max2} > V_{max1}$, data for a two-site model can also be fit to a dual-enzyme model (Korzekwa et al., 1998). Therefore, CYP3A4 data were also fit to eq. 1. A more complicated model, in which two substrates bind cooperatively to two binding sites (Korzekwa et al., 1998; Shou et al., 1999), was not evaluated.

All data were modeled by nonweighted nonlinear regression analysis using SigmaPlot 5.05 (SPSS, Chicago, IL). The goodness of fit of each model was determined by Akaike's information criterion (AIC) or F ratio test (Boxenbaum et al., 1974; Imbimbo et al., 1991). All results are expressed as the mean $\pm$ S.D. of three experiments without specific notation. Statistical analyses to compare the amount of remaining LAAM, formed nor-LAAM, and dinor-LAAM with and without TAO were carried out using unpaired t test with SigmaStat 2.03 (SPSS).

Results

***N*-Demethylation of LAAM and Nor-LAAM by Human Liver Microsomes and Effect of CYP Isoform-Selective Inhibitors.** Formation of both nor-LAAM and dinor-LAAM from LAAM and dinor-LAAM from nor-LAAM was linear with microsomal protein content up to 0.2 mg and incubation time up to 20 min under substrate concentrations tested (data not shown). In addition, less than 10% of the substrate was consumed during incubations. Relationships between formation rates of metabolites and substrate concentration showed hyperbolic saturation kinetics (Fig. 1). Dinor-LAAM concentrations were approximately one-tenth those of nor-LAAM when LAAM was the substrate. Eadie-Hofstee plots were biphasic and concave hyperbolic (versus parabolic), indicating apparent multienzyme kinetics (Fig. 1, insets). Kinetic parameters for the formation of nor-LAAM and dinor-LAAM were obtained by nonlinear regression analysis of metabolite versus substrate data, using a dual-enzyme Michaelis-Menten model. High-affinity K_m (K_{m1}) values for the formation of nor-LAAM from LAAM and dinor-LAAM from nor-LAAM were comparable among liver microsomes from three individuals (HLM135, 158, and 167) (Table 1). The apparent K_{m1} and high-affinity V_{max} (V_{max1}) for dinor-LAAM formation from nor-LAAM were lower than those for nor-LAAM from LAAM in each of these microsomes. The low-affinity K_m (K_{m2}) for nor-LAAM from LAAM and dinor-

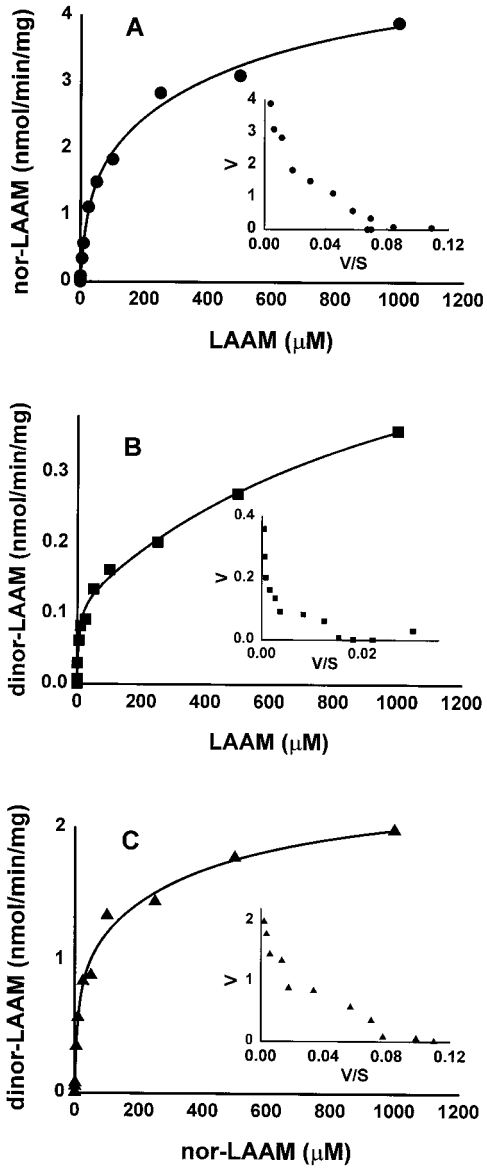

Fig. 1. Relationships between concentrations of LAAM and rates of formation of nor-LAAM (A) and dinor-LAAM (B), and between concentrations of nor-LAAM and rates of formation of dinor-LAAM (C), by human liver microsomes (HLM135). Concentrations of substrates were 0.05 to 1000 μM. Lines represent rates predicted using Michaelis-Menten kinetic parameters derived from nonlinear regression analysis of the expressed data. The insets show Eadie-Hofstee plots for *N*-demethylation of LAAM (A and B) and nor-LAAM (C). Each plot depicts the mean of duplicate experiments.

LAAM from nor-LAAM was 10 times higher than that of K_{m1}. The in vitro clearance estimate ($CL_{int} = V_{max}/K_m$) for the low-affinity enzyme was <10% of that for the high-affinity enzyme. For the high-affinity enzyme, CL_{int} for nor-LAAM from LAAM and dinor-LAAM from nor-LAAM were of the same order of magnitude (0.07 and 0.11 ml/min/mg, respectively).

Of the CYP isoform-specific inhibitors examined, CYP3A4 inhibitors, TAO, erythromycin, ketoconazole, and midazolam inhibited the formation of nor-LAAM from LAAM by more than 50% (Fig. 2). Orphenadrine, paclitaxel, and diclofenac and DDC also decreased the formation of nor-LAAM by approximately 30%. The same profiles of inhibition were ob-

TABLE 1
Kinetic parameters for *N*-demethylation of LAAM and nor-LAAM by human liver microsomes and cDNA-expressed CYP isoforms
Kinetic parameters were obtained using a single-enzyme Michaelis-Menten model for CYP2B6 and a dual-enzyme Michaelis-Menten model for HLM135, 158, 167, and CYP3A4.

	Nor-LAAM from LAAM					Dinor-LAAM from LAAM					Dinor-LAAM from Nor-LAAM				
	K_{m1}	V_{max1}	V_{max1}/K_{m1}	K_{m2}	V_{max2}	K_{m1}	V_{max1}	V_{max1}/K_{m1}	K_{m2}	V_{max2}	K_{m1}	V_{max1}	V_{max1}/K_{m1}	K_{m2}	V_{max2}
	μM	*nmol/min/mg*		*μM*	*nmol/min/mg*	*μM*	*nmol/min/mg*		*μM*	*nmol/min/mg*	*μM*	*nmol/min/mg*		*μM*	*nmol/min/mg*
HLM135	23.0	1.8	0.08	569	3.3	4.9	0.12	0.02	1225	0.54	6.5	0.87	0.13	268	1.4
HLM158	16.2	1.3	0.08	219	1.6	2.6	0.03	0.01	1339	0.44	1.4	0.17	0.12	426	2.3
HLM167	19.1	0.7	0.04	1018	2.6	1.7	0.02	0.01	3783	0.70	3.9	0.37	0.09	667	2.6
	μM	*nmol/min/nmol*		*μM*	*nmol/min/nmol*	*μM*	*nmol/min/nmol*		*μM*	*nmol/min/nmol*	*μM*	*nmol/min/nmol*		*μM*	*nmol/min/nmol*
CYP2B6	17.7	6.8	0.38			4.4	3.18	0.73			26.0	1.63	0.06		
CYP3A4	5.9	2.7	0.46	1247	36.3	1.0	0.38	0.39	2773	2.31	0.2	0.35	1.42	528	11.0

K_{m1}, K_{m2}, Michaelis-Menten constants; V_{max1}, V_{max2}, maximum metabolic velocity.

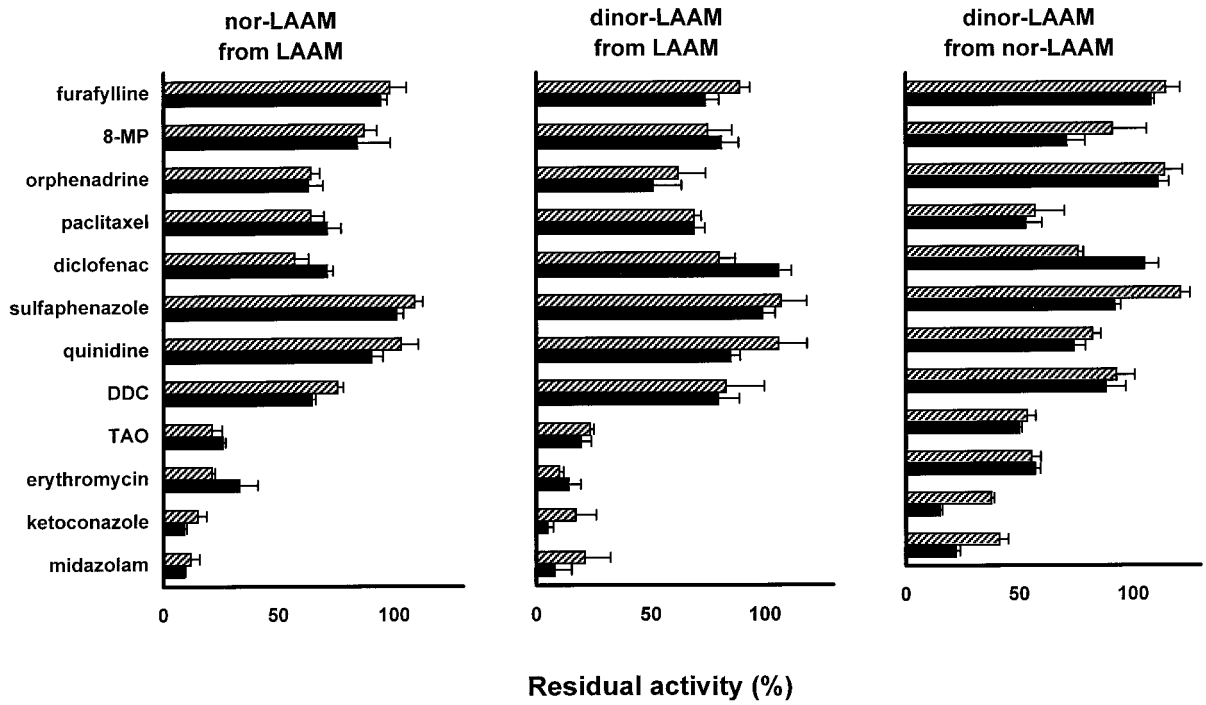

Fig. 2. Effects of CYP isoform-selective inhibitors on the formation of nor-LAAM from LAAM, dinor-LAAM from LAAM, and dinor-LAAM from nor-LAAM by HLM158 (■) and HLM167 (▨). Rates of formation of metabolites were expressed as a percentage of control values without inhibitors obtained from three experiments. Incubations were carried out with the substrates (5 μM), microsomes containing 0.1 mg of protein, inhibitors, and NADPH generating system. Final concentrations of each inhibitor are described under *Materials and Methods*. Uninhibited rates of formation of nor-LAAM and dinor-LAAM from LAAM and dinor-LAAM from nor-LAAM by HLM158 were 243, 8.9, and 145 pmol/min/mg of protein, respectively. Rates of formation of nor-LAAM and dinor-LAAM from LAAM and dinor-LAAM from nor-LAAM by HLM167 were 148, 4.6, and 75 pmol/min/mg of protein, respectively. Data are the mean ± S.D. of three experiments.

served in the formation of dinor-LAAM from LAAM. Other inhibitors did not affect the formation of nor-LAAM or dinor-LAAM from LAAM. TAO, erythromycin, ketoconazole, and midazolam also inhibited the formation of dinor-LAAM from nor-LAAM by approximately 50%. However, neither orphenadrine nor DDC inhibited the formation of dinor-LAAM from nor-LAAM. Paclitaxel, diclofenac, and sulfaphenazole are competitive inhibitors of CYP2C8, 2C8/9, and 2C9, respectively, and inhibit more than 70% of enzyme activity at the concentrations similar to those used in the present study (Mancy et al., 1996; Nadin and Murray, 1999). LAAM metabolism to nor-LAAM was somewhat diminished by paclitaxel, however, inhibition by diclofenac and sulfaphenazole of LAAM and nor-LAAM metabolism was minimal in both microsomes (HLM158 and HLM167), suggesting that the contribution of CYP2C8 and 2C9 to the metabolism of LAAM and nor-LAAM is small.

Metabolism of LAAM and Nor-LAAM by cDNA-Expressed CYP Isoforms. Formation of both nor-LAAM and dinor-LAAM was linear with CYP content up to 10 pmol and incubation time up to 30 min under substrate concentrations tested. Of the representative CYP isoforms in human liver examined, CYP2B6, 2C8, and 3A4 had significantly greater *N*-demethylase activity toward 2 μM LAAM and nor-LAAM, at which concentration the high-affinity enzyme would predominate. This LAAM concentration is near that found in vivo (<1 μM) (Walsh et al., 1998). LAAM and nor-LAAM *N*-demethylation by CYP3A4 was comparable with and without coexpressed cytochrome b_5. CYP3A5 had very low activity toward LAAM and nor-LAAM (Fig. 3). Isoform activity was similar at a substrate concentration of 250 μM, chosen to evaluate the low-affinity component of metabolism, with CYPs 3A4 and 2B6 predominating. *N*-Demethylation of LAAM by CYP2C8 and 2C19 was detected at a substrate concentration of 250 μM, although rates were much lower than those by CYP2B6 and 3A4 (Fig. 3). These results, com-

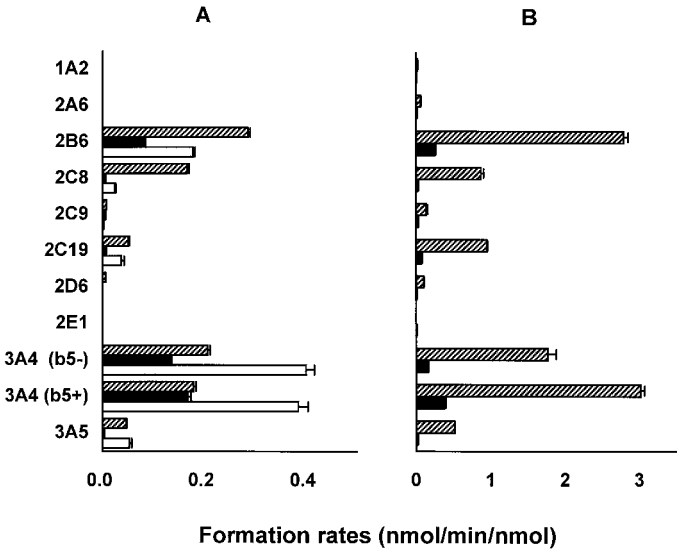

Fig. 3. Rates of formation of nor-LAAM from LAAM (▨), dinor-LAAM from LAAM (■), and dinor-LAAM from nor-LAAM (□) by cDNA-expressed CYP isoforms at a substrate concentration 2 μM (A) and 250 μM (B). Incubations were carried out with substrates, CYP isoforms (10 pmol), and NADPH generating system. b5(+), CYP3A4 expressed with cytochrome b_5; b5(−), CYP3A4 expressed without cytochrome b_5. Data are the mean ± S.D. of three experiments. Formation of dinor-LAAM from nor-LAAM was measured at a substrate concentration of 2 μM only.

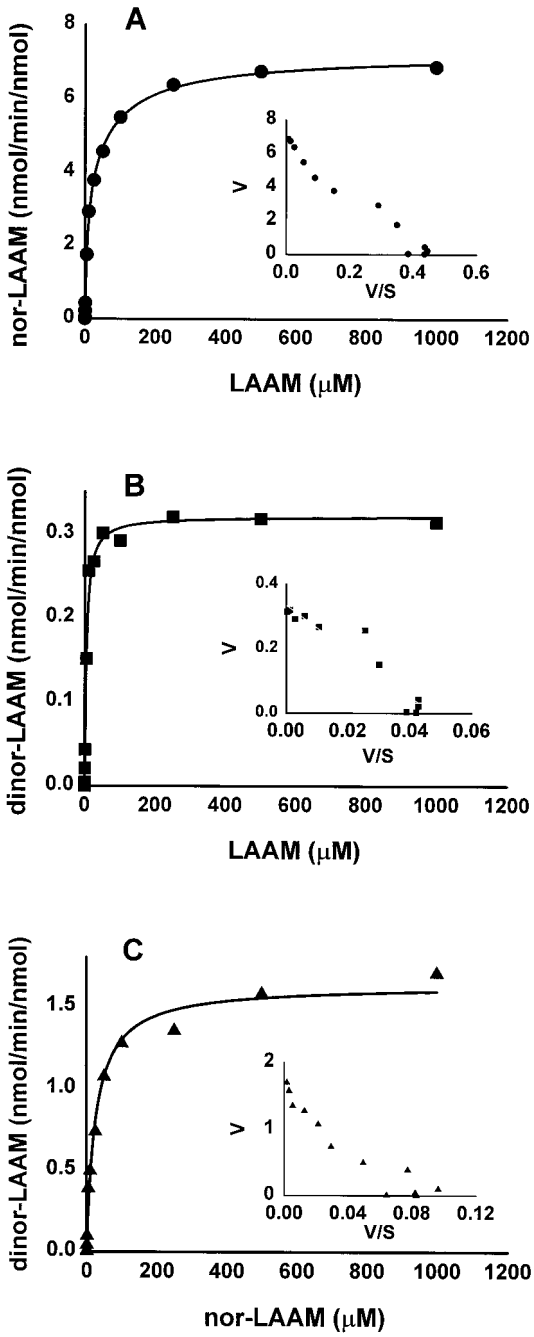

Fig. 4. Relationships between concentrations of LAAM and rates of formation of nor-LAAM (A), dinor-LAAM (B), and between concentrations of nor-LAAM and rates of formation of dinor-LAAM (C) by cDNA-expressed CYP2B6. Concentrations of substrates were 0.05 to 1000 μM. Incubation was carried out in an incubation mixture containing substrates, cDNA-expressed CYP2B6 (10 pmol), and NADPH generating system for 30 min. Each plot depicts the mean of duplicate experiments. Lines represent rates predicted using Michaelis-Menten kinetic parameters derived from nonlinear regression analysis of the data. The insets show Eadie-Hofstee plots for *N*-demethylation of LAAM and nor-LAAM.

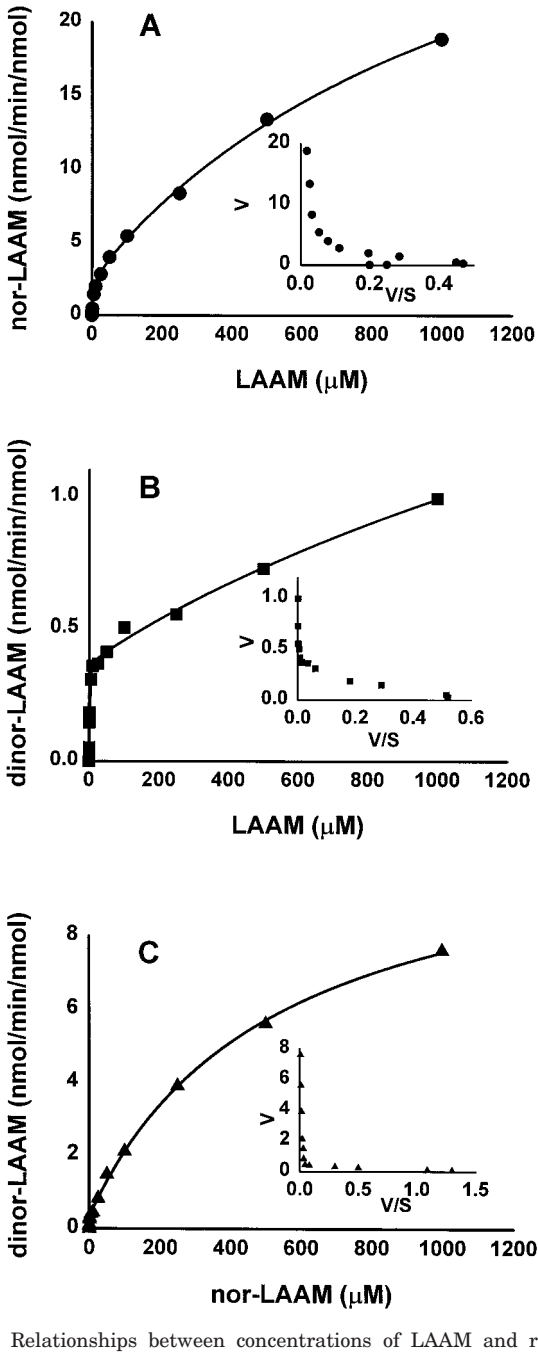

Fig. 5. Relationships between concentrations of LAAM and rates of formation of nor-LAAM (A), dinor-LAAM (B), and between concentrations of nor-LAAM and rates of formation of dinor-LAAM (C) by cDNA-expressed CYP3A4. Concentrations of substrates were 0.05 to 1000 μM. Incubation was carried out in an incubation mixture containing substrates, cDNA-expressed CYP3A4 (10 pmol), and NADPH generating system for 30 min. Each plot depicts the mean of duplicate experiments. Lines represent rates predicted using Michaelis-Menten kinetic parameters derived from nonlinear regression analysis of the expressed data. The insets show Eadie-Hofstee plots for *N*-demethylation of LAAM and nor-LAAM.

bined with those obtained with CYP isoform-selective chemical inhibitors, suggest the possibility that CYP2B6 and/or CYP3A4 are involved in the metabolism of LAAM and nor-LAAM.

Plots of metabolite formation versus substrate concentration for *N*-demethylation of LAAM and nor-LAAM by CYP2B6 showed saturable hyperbolic curves, and Eadie-Hofstee plots showed monophasic kinetics (Fig. 4). Metabolite formation data were fit to a single-enzyme Michaelis-Menten equation. K_m and V_{max} for LAAM *N*-demethylation by CYP2B6 were similar to the high-affinity values obtained with microsomes (Table 1). Analysis using a dual-enzyme model did not improve the fit of the data compared with that using a single enzyme model, as determined by AIC or *F* ratio test.

TABLE 2

Regression analysis for non-Michaelis-Menten saturation curve of *N*-demethylation of LAAM and nor-LAAM by CYP3A4

Values in the parentheses are standard error for each parameter. Equations corresponding to each model are described under *Materials and Methods*. AIC and *F* values were not calculated for modified two-sites models (eqs. 4 and 5) since S.E. was 0 for dinor-LAAM from LAAM and nor-LAAM.

Metabolites and Kinetic Models	K_{m1}	V_{max1}	K_{m2}	V_{max2}	V_{max2}/K_{m2}	K'	V_{max}	n	r	S.E.	AIC	F
Nor-LAAM from LAAM												
Dual-enzyme Michaelis-Menton model (eq. 1)	5.9 (1.8)	2.7 (0.3)	1247 (169)	36.3 (2.5)					>0.99	0.18	−8.3	
Allosteric model (Hill equation) (eq. 2)						2121 (161)	1688 (220)	0.53 (0.04)	>0.99	0.29	4.0	19**
Two-site model (eq. 3)	5.9 (1.7)	2.9 (0.3)	1253 (170)	39.1 (2.7)					>0.99	0.18	−8.3	
Modified two-site model ($K_{m2} \gg K_{m1}$ and $S \ll K_{m2}$) (eq. 4)	32.6 (13.1)	6.4 (0.9)			0.014 (<0.01)				>0.99	0.47	16.4	61**
Modified two-site model ($V_{max1} = 0$) (eq. 5)	<0.01 (6.3)		425 (114)	25.9 (3.0)					0.99	0.97	52.6	94**
Dinor-LAAM from LAAM												
Dual-enzyme Michaelis-Menten model (eq. 1)	1.0 (0.2)	0.4 (0.01)	2773 (1496)	2.3 (0.92)					>0.99	0.02	−64.8	
Allosteric model (Hill equation) (eq. 2)						82 (10)	13.2 (3.0)	0.26 (0.02)	0.98	0.0564	−45.5	37**
Two-site model (eq. 3)	1.0 (0.2)	0.4 (0.01)	2774 (1496)	2.7 (0.93)					>0.99	0.02	−64.8	
Modified two-site model ($K_{m2} \gg K_{m1}$ and $S \ll K_{m2}$) (eq. 4)	1.1 (0)	0.4 (0)			0.0006 (0)				1	0		
Modified two-site model ($V_{max1} = 0$) (eq. 5)	<0.01 (3.3)		18 (11)	0.7 (0.09)					0.90	0.14	−2.3	91**
Dinor-LAAM from nor-LAAM												
Dual-enzyme Michaelis-Menten model (eq. 1)	0.2 (0.2)	0.4 (0.05)	528 (36)	11.0 (0.3)					>0.99	0.08	−29.8	
Allosteric model (Hill equation) (eq. 2)						191 (22)	18.7 (4.0)	0.71 (0.05)	>0.99	0.12	−20.5	12**
Two-site model (eq. 3)	0.2 (0.3)	0.4 (0.05)	528 (36)	11.0 (0.3)					>0.99	0.08	−29.8	
Modified two-site model ($K_{m2} \gg K_{m1}$ and $S \ll K_{m2}$) (eq. 4)	163 (0)	5.7 (0)			0.0032 (0)				1	0		
Modified two-site model ($V_{max1} = 0$) (eq. 5)	<0.01 (3.3)		393 (57)	10.4 (0.6)					>0.99	0.22	22.8	29**

K', binding constant (μM); K_{m1}, K_{m2}, Michaelis-Menten constants (μM); V_{max}, V_{max1}, V_{max2}, maximum metabolic velocity (nmol/min/nmol of P450); V_{max2}/K_{m2} (ml/min/nmol of P450); n, number of binding sites; r, coefficient of regression; S.E., standard error of estimate; F, F ratio.

** $p < 0.01$ compared with a dual-enzyme Michaelis-Menten model and the two-site model.

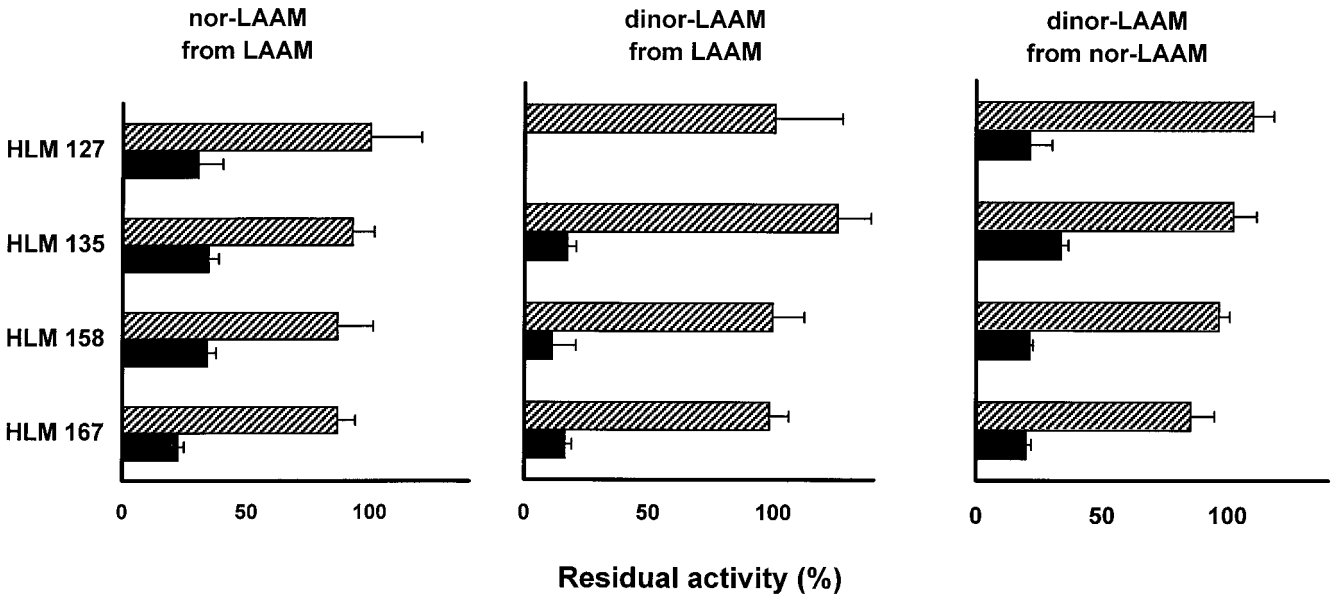

Fig. 6. Effect of monoclonal antibody against CYP2B6 (▨) and troleandomycin (100 μM), a selective CYP3A4 isoform inhibitor (■) on the formation of nor-LAAM from LAAM, dinor-LAAM from LAAM, and dinor-LAAM from nor-LAAM by human liver microsomes from four individuals (HLM127, 135, 158, and 167). Concentration of substrate was 1 μM. Reaction conditions are described under *Materials and Methods*. Contents of protein in antibody and microsomes were 0.02 and 0.05 mg, respectively. Formation of dinor-LAAM from LAAM by HLM127 was completely inhibited by TAO. Rates of formation of metabolites were expressed as a percentage of control mixtures with the solvent of antibody or methanol obtained from three experiments. Rates of formation of nor-LAAM from LAAM, dinor-LAAM from LAAM, and dinor-LAAM from nor-LAAM in control mixture were 13.9, 1.0, and 9.7 pmol/min/mg of protein, respectively, by HLM127; 135.3, 8.4, and 110.9 pmol/min/mg of protein, respectively, by HLM135; 79.8, 5.6, and 45.1 pmol/min/mg of protein, respectively, by HLM158; and 78.6, 4.4, and 55.9 pmol/min/mg of protein, respectively, by HLM167.

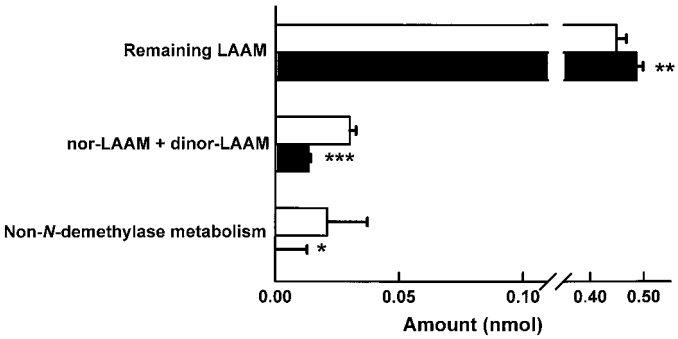

Fig. 7. Content of remaining LAAM, sum of formed nor-LAAM and dinor-LAAM, and non-*N*-demethylase metabolites by HLM135 in the control (□) and TAO (■) groups. Incubations (0.5 ml) were carried out with LAAM (1 μM), microsomes containing 0.2 mg of protein, troleandomycin (100 μM), and NADPH generating system for 10 min. Data are the mean ± S.D. of six experiments. $^{*}p < 0.05$, $^{**}p < 0.01$, $^{***}p < 0.001$ compared with values in the control group.

LAAM and nor-LAAM demethylation by expressed CYP3A4 is shown in Fig. 5. Formation of nor-LAAM and dinor-LAAM was hyperbolic with respect to LAAM concentration, but was not saturable, even at 1 mM substrate. In contrast to CYP2B6, Eadie-Hofstee plots for expressed CYP3A4 were biphasic and concave hyperbolic, indicating apparent non-Michaelis-Menten multisite kinetics with this single isoform. Results were analyzed using a dual-enzyme Michaelis-Menten model, a general allosteric model, and single enzyme two-site models (Table 2). The best fits were obtained using a dual-enzyme or a two-site model (eq. 1 and 3, respectively), with both models giving nearly identical results. There were no differences in the standard error of estimate, coefficient of regression, or AIC between these models, suggesting that fitting of the measured values was comparable. The apparent high affinity K_m (K_{m1}) for nor-LAAM from LAAM and dinor-LAAM from nor-LAAM by CYP3A4 calculated with dual-enzyme Michaelis-Menten model was lower than that obtained by human liver microsomes and by CYP2B6 (Table 1). Nevertheless, this estimate may be artificially reduced by the inability to accurately estimate the K_m for the low-affinity site.

With the modified two-site model assuming $K_{m2} \gg K_{m1}$ and $S \ll K_{m2}$ (eq. 4) or assuming $V_{max1} = 0$ (eq. 5), the fits were poorer ($p < 0.01$ by F ratio test), with larger standard error of the estimates and AIC and smaller coefficients of regression than those with the full two-site model. The Hill equation yielded $n < 1$ for nor-LAAM and dinor-LAAM from LAAM and dinor-LAAM from nor-LAAM. Compared with either the dual-enzyme or two-site models, fitting of the data with the Hill equation (eq. 2) yielded a less satisfactory result ($p < 0.01$).

Effect of Monoclonal Antibody against CYP2B6 and Troleandomycin on the Metabolism of LAAM and Nor-LAAM. For elucidating the contribution of CYP2B6 versus CYP3A4 to the metabolism of LAAM and nor-LAAM in human liver microsomes, we added a monoclonal antibody against CYP2B6 to microsomes obtained from four individuals (HLM127, 135, 158, and 167). CYP2B6 antibody had no effect on the metabolism of LAAM or nor-LAAM. In contrast, CYP2B6 monoclonal antibody (at 0.5 mg/mg of protein) did inhibit LAAM *N*-demethylation by expressed CYP2B6. In contrast to the antibody, TAO inhibited the metabolism of LAAM and nor-LAAM by all of these microsomes by more than 70% (Fig. 6), which is consistent with the results shown in Fig. 2. These data suggest that CYP3A4, not CYP2B6, is predominantly involved in the metabolism of LAAM and nor-LAAM in these microsomes.

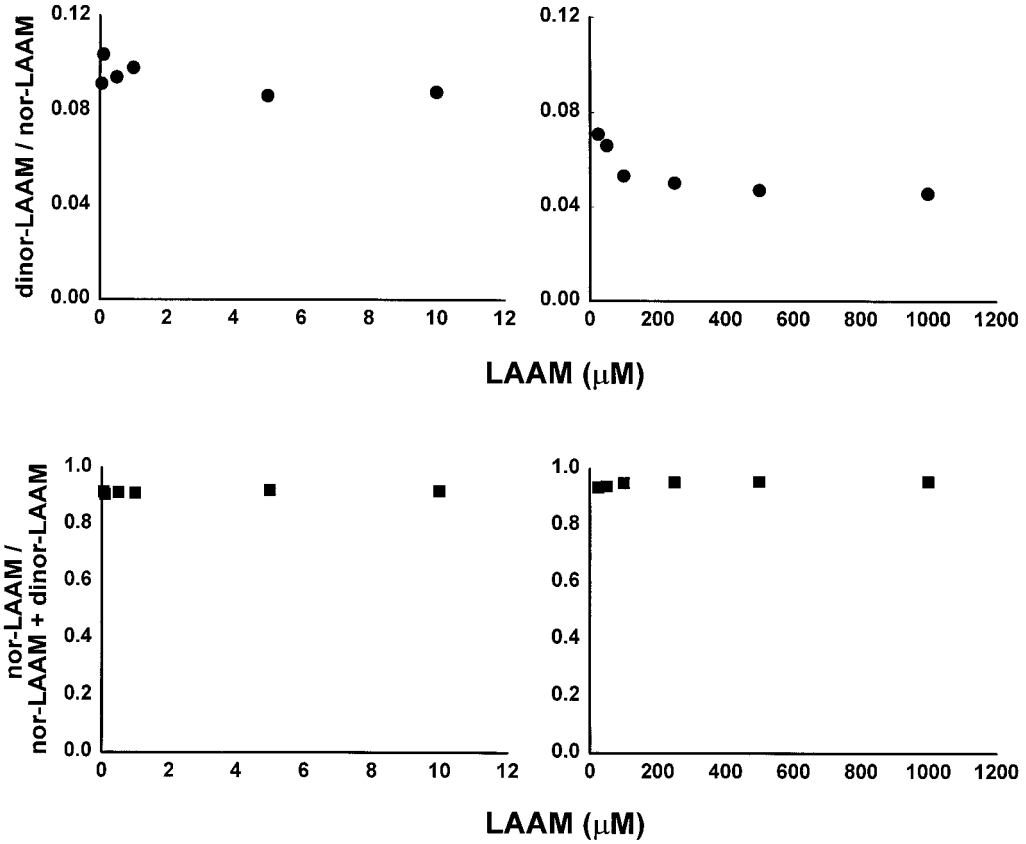

Fig. 8. Ratio of concentration of dinor-LAAM to nor-LAAM (top) and nor-LAAM to the sum of nor-LAAM and dinor-LAAM (bottom) versus concentration of LAAM for CYP2B6. Concentrations of LAAM were 0.05 to 10 (left) and 25 to 1000 μM (right).

Compared with *N*-demethylation, less is known about LAAM metabolism by other routes. Metabolism by non-*N*-demethylation routes (added LAAM minus the sum of remaining LAAM, nor-LAAM, and dinor-LAAM, 21 pmol) was comparable to *N*-demethylation (nor-LAAM plus dinor-LAAM formation, 30 pmol in an incubation containing 500 pmol of LAAM) (Fig. 7). TAO almost completely inhibited non-*N*-demethylated metabolites formation (<1 pmol), suggesting that CYP3A4 also catalyzes these other metabolic pathways. The estimates were not influenced by further metabolism of dinor-LAAM, because disappearance of dinor-LAAM from the incubation mixture was not detected following incubation with microsomes and NADPH for 20 min.

Mechanism of Sequential Metabolism of LAAM to Nor-LAAM and Dinor-LAAM. Two different kinetic mechanisms have been suggested for sequential reactions by CYP (Sugiyama et al., 1994). In mechanism 1, the primary metabolite-enzyme complex is activated and converted to the secondary metabolite before it is released from the enzyme. In mechanism 2, most of the secondary metabolite is formed from primary metabolite that is released and then reassociates with the enzyme to subsequently form the secondary metabolite. Mechanism 1 is characterized by a constant ratio of the secondary to the primary metabolite, and mechanism 2 by a decreased ratio of the secondary to the primary metabolite, respectively, with increasing substrate concentration. The fraction of primary metabolite converted to the secondary metabolite from both released and retained primary metabolite is given by the ratio of secondary metabolite to the sum of primary and secondary metabolites. The fraction of the secondary metabolite formed specifically from the released primary metabolite-enzyme complex can be approximated by the ratio of the concentration of the primary metabolite divided by the sum of the concentrations of the primary and secondary metabolites (Sugiyama et al., 1994).

The fraction of primary metabolite converted by either mechanism was low (<0.1) for CYP2B6, and for CYP3A4 and microsomes at high LAAM concentrations, and higher (0.3–0.8) at low (<1 μM) LAAM concentrations (data not shown). The dinor-LAAM/nor-LAAM ratio was relatively unchanged with increasing substrate concentration in CYP2B6 experiments, but diminished with microsomes and 3A4 (Figs. 8–10, top). For microsomes and CYP3A4, this suggests that dinor-LAAM is formed by mechanism 2 (release and reassociation). The ratio nor-LAAM/(nor-LAAM + dinor-LAAM) was >0.9 in experiments with CYP2B6 throughout the range of LAAM concentrations (Fig. 8, bottom). In contrast, the ratio was <0.5 at LAAM concentrations <0.5 μM but increased to >0.8 at 75 μM LAAM, for both CYP3A4 and microsomes (Figs. 9 and 10, bottom). This suggests more complex kinetics, with most of the dinor-LAAM formed from the nor-LAAM-CYP3A4 complex at low (therapeutic) substrate concentrations, and by the release-reassociation mechanism at higher LAAM concentrations.

Discussion

Several lines of evidence obtained suggest that CYP3A4 is the principal isoform involved in the metabolism of LAAM and nor-LAAM, at both low (therapeutic, <1 μM) and high concentrations. This includes 1) metabolism of LAAM and nor-LAAM by human liver microsomes was significantly inhibited by all CYP3A4-selective chemical inhibitors examined; 2) at both low and high substrate concentrations,

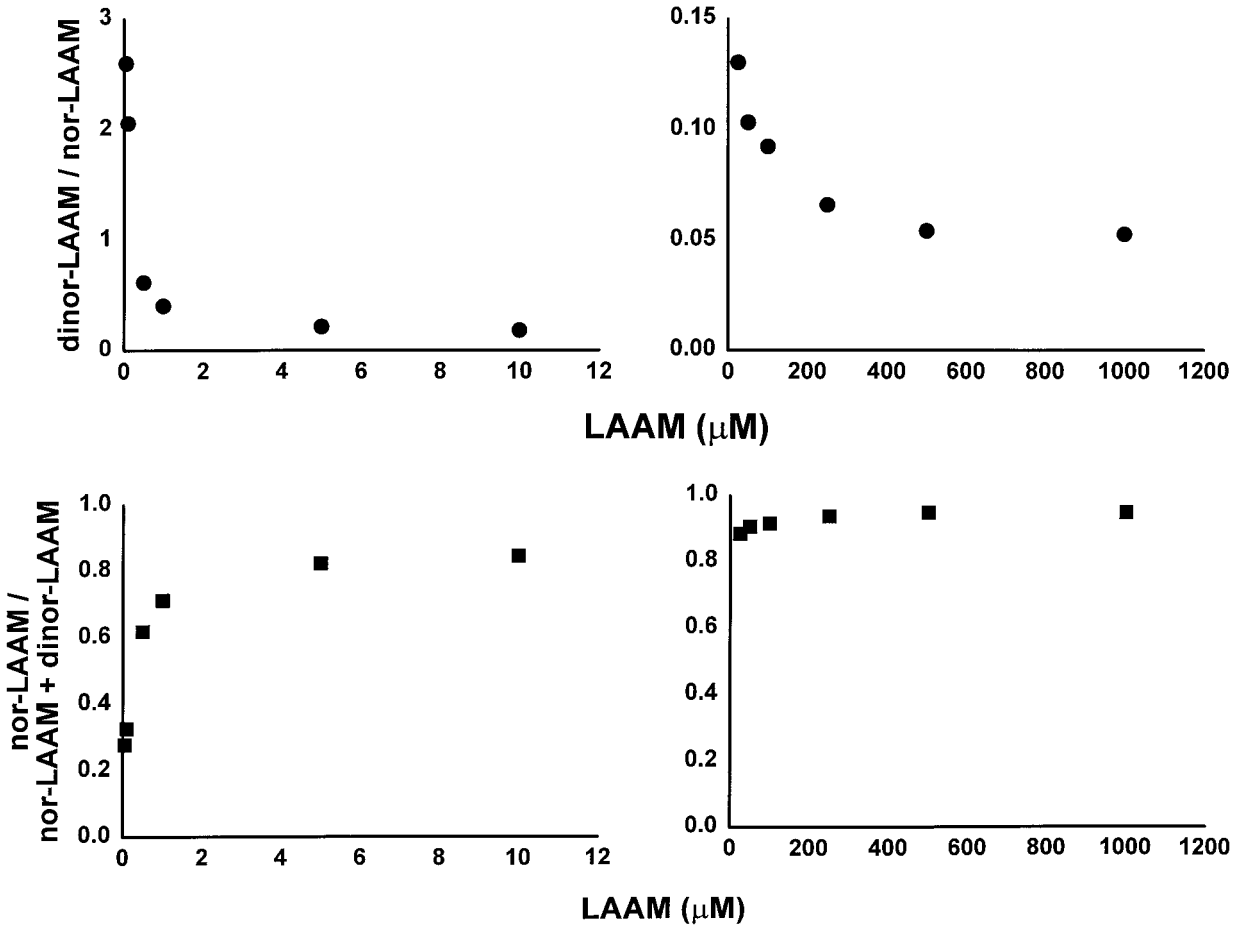

Fig. 9. Ratio of concentration of dinor-LAAM to nor-LAAM (top) and nor-LAAM to the sum of nor-LAAM and dinor-LAAM (bottom) versus concentration of LAAM for CYP3A4. Concentrations of LAAM were 0.05 to 10 (left) and 25 to 1000 μM (right). Vertical scales of the right figures are smaller than those on the left.

CYP3A4 had the highest catalytic activity of any expressed CYP toward LAAM and nor-LAAM; 3) *N*-demethylation of LAAM and nor-LAAM by human liver microsomes showed apparent multienzyme kinetics that was consistent with the multisite kinetics shown by cDNA-expressed CYP3A4 alone; and 4) CYP2B6 monoclonal antibody, which inhibited CYP2B6-catalyzed metabolism of LAAM of LAAM and nor-LAAM, had no effect on human liver microsomal metabolism of LAAM and nor-LAAM at therapeutic concentrations.

Although CYP3A4 is the predominant isoform, CYP2B6 may participate in livers with high levels of CYP2B6 expression. Previous investigators reported CYP2B6 content to be less than 1% of the total CYP in liver (Shimada et al., 1994); however, a recent report using antibody raised against purified recombinant CYP2B6 has shown that CYP2B6 is about 1 to 4% of the total CYP in liver (Hanna et al., 2000). CYP2B6 has significant metabolic activity toward some substrates thought to be catalyzed predominantly by CYP3A4, such as midazolam and dextromethorphan (Ekins et al., 1998; Wang and Unadkat, 1999). In the present study, cDNA-expressed CYP2B6 did metabolize LAAM and nor-LAAM, at rates equal to that of CYP3A4 and with a greater intrinsic clearance, and orphenadrine did inhibit LAAM *N*-demethylation. However orphenadrine inhibits CYP3A4-catalyzed drug metabolism with inhibition constants similar to CYP2B6 (Guo et al., 1997; Sai et al., 2000), suggesting that decreased CYP3A4 activity by orphenadrine could be responsible for the inhibition of metabolism of LAAM and nor-LAAM by orphenadrine. Furthermore, monoclonal antibody against CYP2B6 did not inhibit *N*-demethylation of either LAAM or nor-LAAM by human liver microsomes. Together, these results suggest that CYP2B6 is not significantly involved in the metabolism of LAAM in human liver microsomes; however, we cannot eliminate the possibility of CYP2B6 involvement in some livers, since there are large interindividual differences in CYP2B6 content, and the content of CYP2B6 in the microsomes used in the present study (HLM127, 135, 158, and 167) is not known. Examination of correlations of metabolic activity between LAAM and CYP2B6 specific activity such as (*S*)-mephenytoin *N*-demethylation and 7-ethoxytrifluoromethylcoumarin *O*-deethylation would be required for further determining the contribution of CYP2B6 to the metabolism of LAAM in human liver microsomes (Heyn et al., 1996; Ekins et al., 1998).

LAAM is sequentially metabolized to nor-LAAM and dinor-LAAM. Two different kinetic mechanisms have been suggested for sequential reactions by CYP, secondary metabolism in the active site and release-reassociation (Sugiyama et al., 1994). There may be mechanistic differences between CYPs 2B6 and 3A4 with respect to sequential LAAM metabolism. The similarity between the kinetic behavior of CYP3A4 and microsomes further implies the predominant

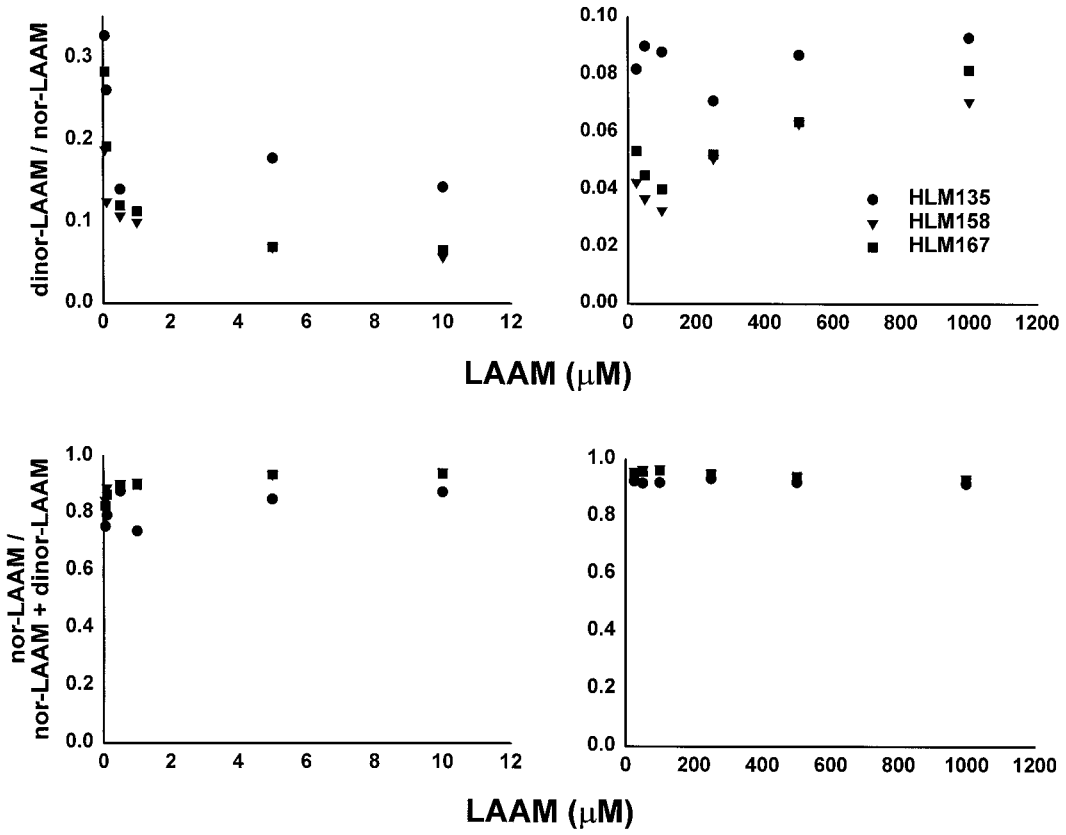

Fig. 10. Ratio of concentration of dinor-LAAM to nor-LAAM (top) and nor-LAAM to the sum of nor-LAAM and dinor-LAAM (bottom) versus concentration of LAAM for human liver microsomes from three individuals (HLM135, 158, and 167). Concentrations of LAAM were 0.05 to 10 (left) and 25 to 1000 μM (right). Vertical scales of the right figures are smaller than those on the left.

contribution of CYP3A4 to the overall metabolism of LAAM to nor-LAAM and dinor-LAAM in human liver microsomes.

Few studies have been performed to elucidate the CYP isoforms involved in the metabolism of LAAM. Moody et al. (1997) found that CYP3A4 was the principal CYP isoform involved in the metabolism of both LAAM and nor-LAAM based on experiments using CYP isoform-selective inhibitors and cDNA-expressed CYP isoforms. Nonetheless, substrate concentrations (10 μM) were at least an order of magnitude higher than therapeutic. CYP2B6 was not included in this analysis and the possibility of the involvement of multiple CYP isoforms was not examined and the kinetic parameters for metabolism of LAAM were not measured. The metabolism of both LAAM and nor-LAAM by human liver microsomes and cDNA-expressed CYP3A4 obtained in the present study is consistent with the report by Moody et al. (1997).

CYP3A4-catalyzed LAAM *N*-demethylation was characterized with microsomes and expressed enzyme (Fig. 5). With both systems, saturation curves were hyperbolic (without apparent sigmoidicity) and Eadie-Hofstee plots were hyperbolic concave. Multiphasic kinetics in microsomes is usually interpreted with a multienzyme model, typically suggesting high-affinity, low-capacity and low-affinity, high-capacity CYPs, each exhibiting Michaelis-Menten kinetics. CYP3A4, however, clearly exhibited non-Michaelis-Menten kinetics, which paralleled the microsomal results, suggesting that the microsomal kinetics derive from non-Michaelis-Menten behavior of CYP3A4 and its predominant role in microsomal LAAM metabolism. Although microsomal data were initially analyzed using the dual-enzyme Michaelis-Menten model, CYP3A4 data yielded similar K_m and V_{max} values with either the dual-enzyme or two-site model, hence microsomal data were not reanalyzed with the latter model.

It is now well established that the CYP3A4 active site contains two or more binding sites, and can accommodate the simultaneous presence of at least two substrate molecules, or one substrate and an allosteric effector (which may be a second substrate molecule) (Shou et al., 1994, 1999; Ueng et al., 1997; Korzekwa et al., 1998; Hosea et al., 2000; Houston and Kenworthy, 2000). Several models have been suggested to rationalize multisite kinetics. If the sites are identical, independent, and have the same substrate affinities, kinetics will be noncooperative, the velocity equation reduces to the simple Michaelis-Menten equation, and Eadie-Hofstee plots are linear. If substrate binding to one site alters the affinity or product formation rate for a second substrate site, then allosterism or homotropic cooperativity results. Positive cooperativity, suggesting substrate activation, is often characterized by sigmoidal velocity curves, parabolic Eadie-Hofstee plots, and a Hill coefficient >1. Negative cooperativity is characterized by hyperbolic velocity and Eadie-Hofstee curves, which are indistinguishable from a dual-enzyme Michaelis-Menten system, and a Hill coefficient <1. Positive homotropic cooperativity with CYP3A4 substrates, with sigmoidal velocity curves, and/or substrate binding, has now been abundantly reported. Nevertheless, no evidence for positive cooperativity with LAAM was observed, because velocity curves and Eadie-Hofstee plots were both hyperbolic. Results were consistent, however, with both a two-site model with $K_{m2} \gg K_{m1}$, and $V_{max2} > V_{max1}$, which does give the aforementioned graphical results (Korzekwa et al., 1998), and a negative cooperativity model. Both models have a Hill

coefficient less than 1. Observed rates were better fit to a two-site model than the Hill equation. Interestingly, results were also well fit to a dual-enzyme model while yielding similar parameters to the two-site model. A unique, identifiable model cannot be specified from the available data. Compared with positive cooperativity, apparent negative cooperativity in CYP3A4-catalyzed metabolism is relatively rare. LAAM may be the third example, in addition to naphthalene and the antiarrhythmic agent BRL32872 (Clarke, 1998; Korzekwa et al., 1998). Further investigation is required to elucidate the mechanism of CYP3A4-catalyzed LAAM metabolism.

Of the two LAAM binding sites, only the high-affinity binding site appears relevant for LAAM metabolism in vivo, since even the high affinity K_m (K_{m1}) for CYP3A4 was higher than plasma concentrations of LAAM and nor-LAAM following intravenous and oral administration (Walsh et al., 1998), and the low affinity K_m (K_{m2}) was substantially higher than in vivo concentrations. The high affinity V_{max} (V_{max1}) for LAAM *N*-demethylation was greater than that for nor-LAAM, consistent with the longer in vivo elimination half-life of nor-LAAM (Billings et al., 1973). Thus, the greater hepatic rate of nor-LAAM formation versus elimination, combined with the 5- to 10-fold greater potency of nor-LAAM compared with LAAM (Horng et al., 1976; Walczak et al., 1981), accounts for the long duration of clinical effect of LAAM.

The present results suggest that in vivo induction of CYP3A4 would increase metabolism of LAAM to nor-LAAM and dinor-LAAM. Since the intrinsic clearances for LAAM and nor-LAAM are similar, and dinor-LAAM is not further metabolized, concentrations of both metabolites would be predicted to increase and enhance LAAM effect, since both metabolites are more potent than LAAM. Using microsomal kinetic parameters and appropriate scaling, the predicted formation clearance of nor-LAAM was 44, 133, and 15 ml/min/kg and that of dinor-LAAM was 14, 42, and 5 ml/min/kg of body weight under control, CYP3A4-induced, and inhibited conditions, respectively. In contrast to this prediction, however, phenobarbital pretreatment decreased plasma concentrations of nor-LAAM and dinor-LAAM as well as LAAM, and decreased LAAM analgesia in animals (Roerig et al., 1977; Kuttab et al., 1985). This cannot be explained by preferential induction of nor-LAAM (versus LAAM) metabolism, or by dinor-LAAM metabolism. Rather, these results suggest that phenobarbital pretreatment induced an alternative metabolic pathway leading to analgesically inactive metabolites. We therefore evaluated non-*N*-demethylase LAAM metabolic pathways in human liver microsomes. Metabolism by non-*N*-demethylase pathways was almost completely inhibited by TAO, suggesting CYP3A4 involvement. CYP3A4 induction in humans might therefore preferentially induce non-*N*-demethylation pathways, diminishing nor-LAAM formation and LAAM clinical effect. The discrepancies between in vivo and in vitro experiments strongly suggest the necessity for pharmacokinetic studies in humans with CYP3A4 inducers and inhibitors for understanding LAAM disposition and interactions.

In summary, we have shown that LAAM and its active metabolite nor-LAAM are predominantly metabolized by CYP3A4 in human liver microsomes and CYP3A4-catalyzed metabolism demonstrates unusual multisite kinetics.

Note Added in Proof. LAAM metabolism by CYP3A4 was also analyzed using a variation of eq. 3, with a single V_{max} and replacement of V_{max2} with $\alpha \cdot V_{max}$, to allow for different rates of metabolism of the ES and ESS complexes (Schrag and Wienkers, 2001). Parameters (K_{m1}, K_{m2}, V_{max}, and $\alpha \cdot V_{max}$) and AIC values were identical to those obtained with eqs. 1 and 3.

Acknowledgment

We thank Carole Jubert, Ph.D., for technical assistance.

References

Billings RE, Booher R, Smits S, Pohland A and McMahon RE (1973) Metabolism of acetylmethadol. A sensitive assay for noracetylmethadol and the identification of a new active metabolite. *J Med Chem* **16:**305–306.
Boxenbaum HG, Riegelman S and Elashoff RM (1974) Statistical estimations in pharmacokinetics. *J Pharmacokinet Biopharm* **2:**123–148.
Carlile DJ, Hakooz N, Bayliss MK and Houston JB (1999) Microsomal prediction of in vivo clearance of CYP2C9 substrates in humans. *Br J Clin Pharmacol* **47:**625–635.
Clarke SE (1998) In vitro assessment of human cytochrome P450. *Xenobiotica* **28:**1167–1202.
Dresser GK, Spence JD and Bailey DG (2000) Pharmacokinetic-pharmacodynamic consequences and clinical relevance of cytochrome P450 3A4 inhibition. *Clin Pharmacokinet* **38:**41–57.
Eissenberg T, Stitzer ML, Bigelow GE, Buchhalter AR and Walsh SL (1999) Relative potency of levo-alpha-acetylmethadol and methadone in humans under acute dosing conditions. *J Pharmacol Exp Ther* **289:**936–945.
Ekins S, Vandenbranden M, Ring BJ, Gillespie JS, Yang TJ, Gelboin HV and Wrighton SA (1998) Further characterization of the expression in liver and catalytic activity of CYP2B6. *J Pharmacol Exp Ther* **286:**1253–1259.
Ekins S and Wrighton SA (1999) The role of CYP2B6 in human xenobiotic metabolism. *Drug Metab Rev* **31:**719–754.
Fraser HF and Isbell H (1952) Actions and addiction liabilities of alpha-acetylmethadols in man. *J Pharmacol Exp Ther* **105:**458–465.
Guo Z, Raeissi S, White RB and Stevens JC (1997) Orphenadrine and methimazole inhibit multiple cytochrome P450 enzymes in human liver microsomes. *Drug Metab Dispos* **25:**390–393.
Hanna IH, Reed JR, Guengerich FP and Hollenberg PF (2000) Expression of human cytochrome P450 2B6 in *Escherichia coli*: Characterization of catalytic activity and expression levels in human liver. *Arch Biochem Biophys* **376:**206–216.
Henderson GL (1976) Pharmacodynamics of LAAM in man: Plasma levels of LAAM and its metabolites following acute and chronic administration in man (fourth and sixth quarter progress reports). 1974–5. *NIDA Res Monogr* 64–65.
Heyn H, White RB and Stevens JC (1996) Catalytic role of cytochrome P4502B6 in the N-demethylation of S-mephenytoin. *Drug Metab Dispos* **24:**948–954.
Horng JS, Smits SE and Wong DT (1976) The binding of optical isomers of methadone, α-acetylmethadol and their *N*-demethylated derivatives to the opiate receptors of rat brain. *Res Commun Chem Pathol Pharmacol* **14:**621–629.
Hosea NA, Miller GP and Guengerich FP (2000) Elucidation of distinct ligand binding sites for cytochrome P450 3A4. *Biochemistry* **39:**5929–5939.
Houston JB (1994) Utility of in vitro drug metabolism data in predicting in vivo metabolic clearance. *Biochem Pharmacol* **47:**1469–1479.
Houston JB and Carlile DJ (1997) Prediction of hepatic clearance from microsomes, hepatocytes, and liver slices. *Drug Metab Rev* **29:**891–922.
Houston JB and Kenworthy KE (2000) In vitro-in vivo scaling of CYP kinetic data not consistent with the classical Michaelis-Menten model. *Drug Metab Dispos* **28:**246–254.
Huang Z, Roy P and Waxman DJ (2000) Role of human liver microsomal CYP3A4 and CYP2B6 in catalyzing N-dechloroethylation of cyclophosphamide and ifosfamide. *Biochem Pharmacol* **59:**961–972.
Imbimbo BP, Martinelli P, Rocchetti M, Ferrari G, Bassotti G and Imbimbo E (1991) Efficiency of different criteria for selecting pharmacokinetic multiexponential equations. *Biopharm Drug Dispos* **12:**139–147.
Kaiko RF and Inturrisi CE (1975) Disposition of acetylmethadol in relation to pharmacologic action. *Clin Pharmacol Ther* **18:**96–103.
Kharasch ED and Thummel KE (1993) Identification of cytochrome P450 2E1 as the predominant enzyme catalyzing human liver microsomal defluorination of sevoflurane, isoflurane, and methoxyflurane. *Anesthesiology* **79:**795–807.
Koenigs LL, Peter RM, Thompson SJ, Rettie AE and Trager WF (1997) Mechanism-based inactivation of human liver cytochrome P450 2A6 by 8-methoxypsoralen. *Drug Metab Dispos* **25:**1407–1415.
Kolars JC, Awni WM, Merion RM and Watkins PB (1991) First-pass metabolism of cyclosporin by the gut. *Lancet* **338:**1488–1490.
Korzekwa KR, Krishnamachary N, Shou M, Ogai A, Parise RA, Rettie AE, Gonzalez FJ and Tracy TS (1998) Evaluation of atypical cytochrome P450 kinetics with two-substrate models: Evidence that multiple substrates can simultaneously bind to cytochrome P450 active sites. *Biochemistry* **37:**4137–4147.
Kuttab SH, Nowshad F and Shargel L (1985) Effect of phenobarbital pretreatment on the plasma and urinary levels of (−)-alpha-acetylmethadol and its metabolites. *J Pharm Sci* **74:**331–334.
Lowry OH, Rosebrough NJ, Farr AL and Randall RJ (1951) Protein measurement with the Folin phenol reagent. *J Biol Chem* **193:**266–275.
Mancy A, Dijols S, Poli S, Guengerich P and Mansuy D (1996) Interaction of sulfaphenazole derivatives with human liver cytochromes P450 2C: Molecular

origin of the specific inhibitory effects of sulfaphenazole on CYP 2C9 and consequences for the substrate binding site topology of CYP 2C9. *Biochemistry* **35:** 16205–16212.
Moody DE, Alburges ME, Parker RJ, Collins JM and Strong JM (1997) The involvement of cytochrome P450 3A4 in the *N*-demethylation of *L*-α-acetylmethadol (LAAM), norLAAM, and methadone. *Drug Metab Dispos* **25:**1347–1353.
Nadin L and Murray M (1999) Participation of CYP2C8 in retinoic acid 4-hydroxylation in human hepatic microsomes. *Biochem Pharmacol* **58:**1201–1208.
Nickander R, Booher R and Miles H (1974) Alpha-1-acetylmethadol and its N-demethylated metabolites have potent opiate action in the guinea pig isolated ileum. *Life Sci* **14:**2011–2017.
Obach RS, Baxter JG, Liston TE, Silber BM, Jones BC, MacIntyre F, Rance DJ and Wastall P (1997) The prediction of human pharmacokinetic parameters from preclinical and in vitro metabolism data. *J Pharmacol Exp Ther* **283:**46–58.
Omura T and Sato R (1964) The carbon monoxide-binding pigment of liver microsomes. II. Solubilization, purification, and properties. *J Biol Chem* **239:**2379–2385.
Paine MF, Shen DD, Kunze KL, Perkins JD, Marsh CL, McVicar JP, Barr DM, Gillies BS and Thummel KE (1996) First-pass metabolism of midazolam by the human intestine. *Clin Pharmacol Ther* **60:**14–24.
Rawson RA, Hasson AL, Huber AM, McCann MJ and Ling W (1998) A 3-year progress report on the implementation of LAAM in the United States. *Addiction* **93:**533–540.
Roerig DL, Hasegawa AT and Wang RI (1977) Effect of alteration of metabolism on the analgesic activity, toxicity, distribution and excretion of l-alpha-acetylmethadol in the rat. *J Pharmacol Exp Ther* **203:**377–387.
Roy P, Tretyakov O, Wright J and Waxman DJ (1999) Stereoselective metabolism of ifosfamide by human P-450s 3A4 and 2B6. Favorable metabolic properties of R-enantiomer. *Drug Metab Dispos* **27:**1309–1318.
Sai Y, Dai R, Yang TJ, Krausz KW, Gonzalez FJ, Gelboin HV and Shou M (2000) Assessment of specificity of eight chemical inhibitors using cDNA-expressed cytochromes P450. *Xenobiotica* **30:**327–343.
Schrag ML and Wienkers LC (2001) Triazolam substrate inhibition: Evidence of competition for heme-bound reactive oxygen within the CYP3A4 active site. *Drug Metab Dispos* **29:**70–75.
Shimada T, Yamazaki H, Mimura M, Inui Y and Guengerich FP (1994) Interindividual variations in human liver cytochrome P450 enzymes involved in the oxidation of drugs, carcinogens and toxic chemicals: Studies with liver microsomes of 30 Japanese and 30 Caucasians. *J Pharmacol Exp Ther* **270:**414–423.
Shou M, Grogan J, Mancewicz JA, Krausz KW, Gonzalez FJ, Gelboin HV and Korzekwa KR (1994) Activation of CYP3A4: Evidence for the simultaneous binding of two substrates in a cytochrome P450 active site. *Biochemistry* **33:**6450–6455.
Shou M, Mei Q, Ettore MW Jr, Dai R, Baillie TA and Rushmore TH (1999) Sigmoidal kinetic model for two co-operative substrate-binding sites in a cytochrome P450 3A4 active site: An example of the metabolism of diazepam and its derivatives. *Biochem J* **340:**845–853.
Smits SE (1974) The analgesic activity of alpha-1-acetylmethadol and two of its metabolites in mice. *Res Commun Chem Pathol Pharmacol* **8:**575–578.
Sugiyama K, Nagata K, Gillette JR and Darbyshire JF (1994) Theoretical kinetics of sequential metabolism in vitro. Study of the formation of 16 alpha-hydroxyandrostenedione from testosterone by purified rat P450 2C11. *Drug Metab Dispos* **22:**584–591.
Ueng Y-F, Kuwabara T, Chun Y-J and Guengerich FP (1997) Cooperativity in oxidations catalyzed by cytochrome P450 3A4. *Biochemistry* **36:**370–381.
Vaupel DB and Jasinski DR (1997) l-alpha-Acetylmethadol, l-alpha-acetyl-*N*-normethadol and l-alpha-acetyl-*N*,*N*-dinormethadol: Comparisons with morphine and methadone in suppression of the opioid withdrawal syndrome in the dog. *J Pharmacol Exp Ther* **283:**833–842.
Walczak SA, Makman MH and Gardner EL (1981) Acetylmethadol metabolites influence opiate receptors and adenylate cyclase in amygdala. *Eur J Pharmacol* **72:**343–349.
Walsh SL, Johnson RE, Cone EJ and Bigelow GE (1998) Intravenous and oral *l-a*-acetylmethadol: Pharmacodynamics and pharmacokinetics in humans. *J Pharmacol Exp Ther* **285:**71–82.
Wang Y and Unadkat JD (1999) Enzymes in addition to CYP3A4 and 3A5 mediate N-demethylation of dextromethorphan in human liver microsomes. *Biopharm Drug Dispos* **20:**341–346.

Send reprint requests to: Dr. Evan D. Kharasch, Department of Anesthesiology, Box 356540, University of Washington, Seattle, WA 98195-6540. E-mail: kharasch@u.washington.edu